SAND2014-15499C

Equation-of-State and Shock Homogeneity of IMX-101 and IMX-104

Michael D. Furnish*, Seth Root*, and Phil Samuels‡

*Dept. 1646, MS 1195, Sandia National Laboratories, PO Box 5800, Albuquerque, NM 87185-1195

‡Phil Samuels, Picatinny Arsenal, NJ 07806-5000, USA

Abstract. IMX-101 and IMX-104 are relatively new (IM) Insensitive Munition explosives intended to replace TNT and Composition B; however, little fundamental equation-of-state data exists for these explosives We report the results of a program of planar-impact experiments on these two explosives initially loaded to stresses ranging from 4.4 to 16.5 GPa. The primary diagnostic, velocimetry (both VISAR and PDV) was used to track the velocity history of the downstream interface between the explosive sample and a sodium chloride window. Each experiment included multiple samples with thicknesses ranging from 3 to 12 mm to allow establishing equation-of-state properties of the unreacted material and run-to-detonation distance as a function of loading. Selected tests used spatially resolved interferometry (line-imaging VISAR or multiple probes) to monitor the spatial dependence of the wave arrival at the window interface, giving information about the heterogeneity of the wavefront in IMX-104.

Introduction

A key goal of munitions improvement is reducing the likelihood of accidental detonation. To this end, the insensitive munitions IMX-101 and IMX-104 have been developed as respective substitutes for TNT and Composition B. The present study focusses on the pre-detonation equation of state of these materials, although run-to-detonation is also investigated.

IMX-101 is composed of 2,4-Dinitroanisole (DNAN), Nitroguandidne (NQ), and 3-Nitro-1,2,4-triazol-5-one (NTO). IMX-104 is composed of DNAN, NTO and RDX. Selected physical properties of these materials are compared with corresponding properties of TNT and Comp-B in Table 1.

Table 1. Selected properties of IMX-101, IMX-104, TNT and Comp-B

Mat'l	Det Vel km/s	Density gm/cm^3	CJ Pressure GPa
IMX-101	6.9	1.60	21.3
IMX-104	7.4	1.75	25.2
TNT	6.9	1.64	18.9
Comp-B	7.98	1.71	29.7

The present IMX-101 and IMX-104 samples contain internal voids up to a few mm in size. The average porosity of the IMX-101 in this study is 3.0%; that of the IMX-104 is 1.4%. This introduces the possibility of data variability depending on void location relative to the points monitored by the experiment diagnostics. We have not radiographed the present samples.

The primary properties of interest for the IMX-101 and IMX-104 discussed in the present paper include the unreacted Hugoniots and loading waves, material heterogenity, and the run-to-detonation properties. The physical properties of the detonation products will be further addressed in a later paper, together with additional run-to-detonation results.

Experiment Design

These experiments utilize the powder-driven gun range at Sandia's STAR Facility (89 mm bore, impact velocities 0.5 - 2.2 km/s) and VISAR velocimetry diagnostics. This affords a supported shock wave, by contrast with the Taylor wave produced by explosive plane-wave lenses.

In recent years, the value of placing multiple samples on a single target has become apparent (Furnish, et al, 2013). This allows the comparison of responses of different samples to identical loading histories; for example, providing waveform evolution information from which material strength properties may be deduced. Of particular interest here is the comparison of IMX-101 or IMX 104 samples of different thicknesses driven at stress levels of 4 - 15 GPa. In this stress region, the loading wave is discontinuous and no strength information is directly available. However, the wave speed may be measured at different sample thicknesses, giving not only Hugoniot information but also information about the run-to-detonation at the experiment pressure.

The initial shots were designed as shown in Fig. 1. There are 4 IMX samples of thicknesses 3, 6, 9 and 12 mm, each 19 mm in diameter, at 90 degree positions 22.9 mm from the center. Each has a LiF or NaCl window mounted to the rear surface. A LiF window at the center is mounted flush with the impact surface, and serves as a time-of-impact diagnostic. PDV[1] was used to monitor the motion of the interface between the NaCl buffer and window for each sample, and VISAR[2] monitors the motion of the front surface of the LiF window at the target center. Self-shorting pins mounted adjacent to each IMX sample at a 41.27 mm radius provide impact tilt information, allowing the calculation of a position-dependent impact tilt correction to the impact time defined by the central LiF window.

The IMX samples (19 mm diameter) were glued into Lexan(R) rings to reduce any edge effects inasmuch as the shock impedance of Lexan is fairly close to that of the IMX.

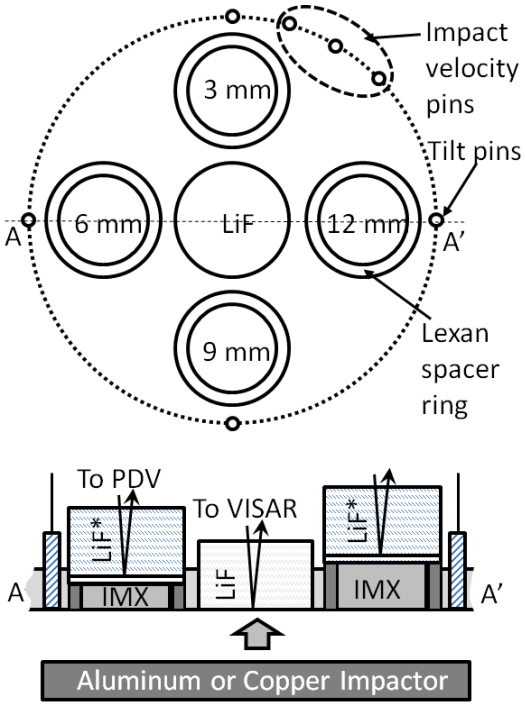

Fig. 1. Configuration of all shots except 104-3 and 104-4. Dimensions are nominal sample thicknesses.
*These windows are NaCl for test 101-5; the buffers are also only used for 101-5.

In view of results of chemical compatibility tests, the present shots were assembled using Epotek® 301 adhesive, a clear binary epoxy with a 24-hour room temperature cure. This compatibility does not extend to TNT or Composition-B.

For the final two shots, a new design was used capitalizing on the availability of a 19-beam VISAR system at the STAR Facility. This system, together with a set of LeCroy WavePro digitizers triggered by a common trigger and also recording a common timemark, allows the recording of 19

time-correlated velocity histories. It was developed by National Security Technologies, LLC[3], improving on an earlier 7-beam design by Barker[2]. The design is show in Fig. 2.

This configuration used 6 flush-mounted LiF windows to map the impact timing, fit to a surface expressed as:

$$t = ax + by + c + dr^2 \qquad \text{Eq. 1}$$

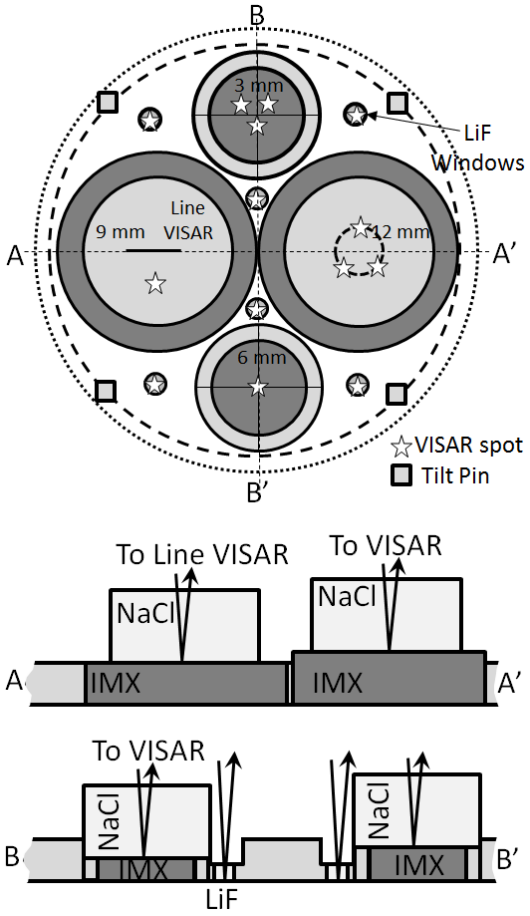

Fig. 2. Configuration for shots 104-3 and 104-4.

The motion of the impact surfaces of these LiF windows was monitored with channels from the same VISAR system used to monitor the motion of the IMX sample rear surfaces, allowing shock transit times to be determined to 1 – 2 ns.

NaCl windows were used instead of LiF, allowing a better mechanical impedance match with the IMX. The impedance match, the product of initial density times zero-pressure sound speed, determines the strength of release or reshock waves sent back into the sample from the window.

Although the figure shows line VISAR used on the 9 mm thick sample, point VISAR was used there on the second shot.

The primary information available from this configuration is:

- Hugoniot data, derived from shock transit times, initial sample density, impact velocity and the Hugoniot of the impactor
- Reshock data, derived from the window Hugoniot and the post-shock velocity of the sample/window interface
- Run-to-detonation distance, deduced from the wavefront arrival times for each thickness.
- Sample heterogeneity, deduced from the spatial variation in the above data.

A total of 5 experiments were conducted with IMX-101 samples, and 4 with IMX-104. Of these, all utilized the geometry of Figure 1 except for the last two IMX-104 experiments. Key parameters are summarized in Table 2.

Table 2. Shot parameters

Shot #	Setup #*	Diag.**	Impactor Matl/thick	Vel km/s
101-1	1	PDV	Al 12.5 mm	0.986
101-2	1	PDV	Al 12.7 mm	1.416
101-3	1	PDV	Al 12.6 mm	2.082
101-4	1	PDV	Cu 9.3 mm	2.032
101-5†	1	VISAR	Cu 8.0 mm	1.983
104-1	1	PDV	Al 12.6 mm	1.460
104-2	1	PDV	Al 12.5 mm	1.629
104-3‡	2	VISAR	Cu 12.7 mm	1.849
104-4	2	VISAR	Cu 12.7 mm	2.034

*Setup number corresponds to fig. numbers
**Refers to the on-sample interferometry. Flush window spots were VISAR throughout.
†1.8 mm NaCl buffer used and NaCl windows
‡ Line VISAR on 9 mm sample

Hugoniot Results

Hugoniot values were determined via the shock transit times. This was established explicitly for shots 101-5, 104-3 and 104-4, in which a common VISAR timebase was used for impact timing and sample/window interface velocimetry. For shots 101-1 through 101-4, a common timebase could not be established between the central LiF window and the other samples, so the timing (corrected for tilt (as indicated by the tilt pins) was adjusted so that the wavespeeds for the 3 and 6 mm thick samples were equal. The procedure for shots 104-1 and 104-2 was similar. The results are listed in Table 3 and plotted in Fig. 3. Initial densities were 1.63 gm/cm^3 for IMX-101 and 1.735 gm/cm^3 for IMX-104.

Table 3. Hugoniot values.

Shot	U_P km/s	U_S km/s	P GPa	ρ gm/cc	ε
101-1	0.7	3.78	4.33	2.003	0.186
101-2	0.97	4.47	7.1	2.082	0.217
101-3	1.36	5.62	12.4	2.150	0.247
101-4	1.64	6.4	15.8	2.258	0.278
101-5	1.58	6.41	16.48	2.160	0.247
104-1	0.98	4.56	7.70	2.194	0.211
104-2	1.10	4.54	8.64	2.289	0.249
104-3	1.50	5.38	14.7	2.402	0.279
104-4	1.64	5.55	15.8	2.460	0.299

Waveforms and Reshock States

Waveforms for the first four IMX 101 shots are shown in Fig. 4. The two lower-velocity shots have relatively level waveforms following the initial loading, although it is interesting that more features are seen on 101-1 than on the higher-velocity 101-2. It is unlikely this is due to sample heterogeneities because similar behavior is seen on all four samples in each shot (excluding the 12 mm sample in 101-2, which did not produce a measurable PDV waveform). The highest pressure shot (101-4) shows a sharp initial peak on the 9 mm sample waveform that resembles a von Neumann spike. However, wavespeed data (discussed in more detail later) suggests that detonation is not occuring in this sample.

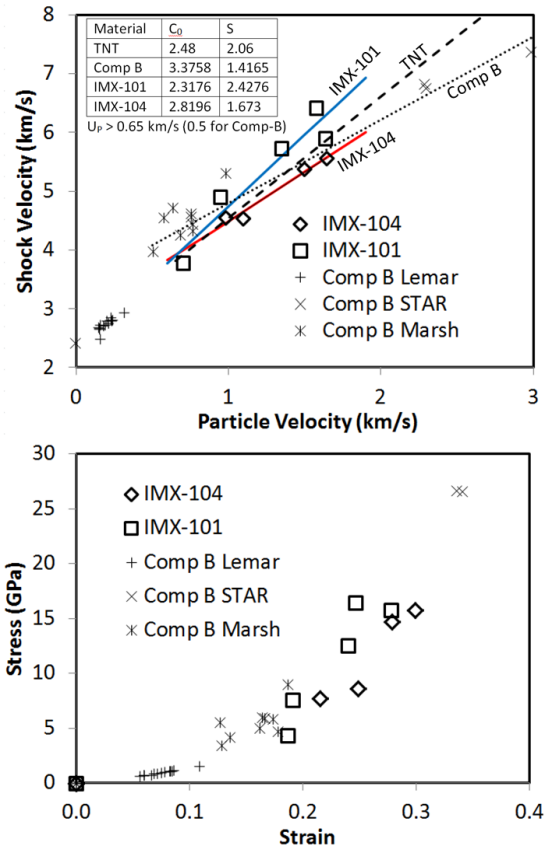

Fig. 3. Hugoniot states for IMX-101 and 104. Comp-B points are from [4-6]; TNT trendline is from [7].

The final IMX-101 test, which used NaCl windows and buffers, produced the waveforms shown in Fig. 5. This test may better represent the in-situ waveforms than tests 101-2 through 101-4 because NaCl is a closer impedance match for IMX-101 (and IMX-104) than is LiF (shown later in Fig. 9). The waveforms from the 6 – 12 mm samples in this 16.5 GPa test show a general relaxing following initial loading, with no clear evidence of detonation.

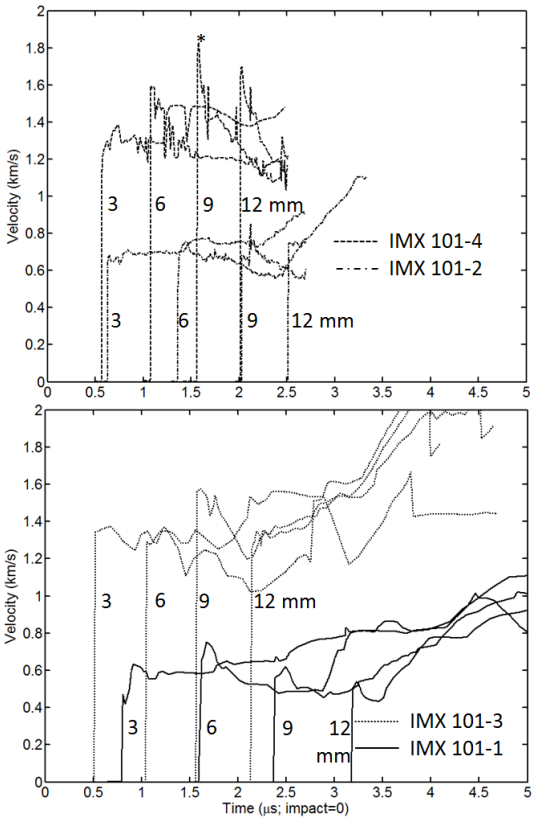

Fig. 4. Waveforms measured by PDV for shots 101-1 through 101-4 (design in Fig. 1).

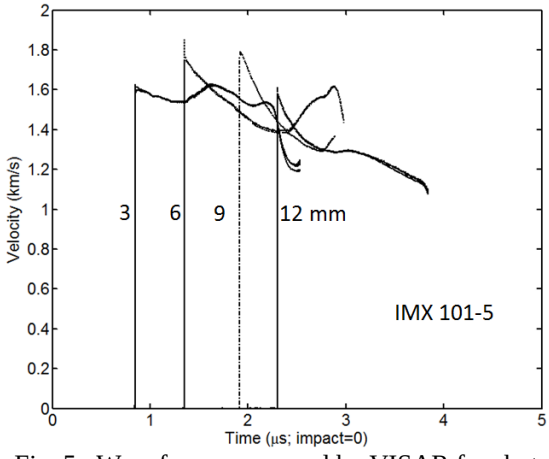

Fig. 5. Waveforms measured by VISAR for shot 101-5 (design in Fig. 1).

The first two of the IMX-104 tests produced the waveforms shown in Fig. 6. These again used LiF windows without buffers, and the resulting waveform features are similar to those observed on the IMX-101 shots with LiF windows. The initial velocity pike on the 12 mm sample in shot 104-2 (8.8 GPa) is unlikely to be a detonation-related feature because the wavespeed does not increase to near the 7.5 km/s expected for a detonation wavefront in IMX-104.

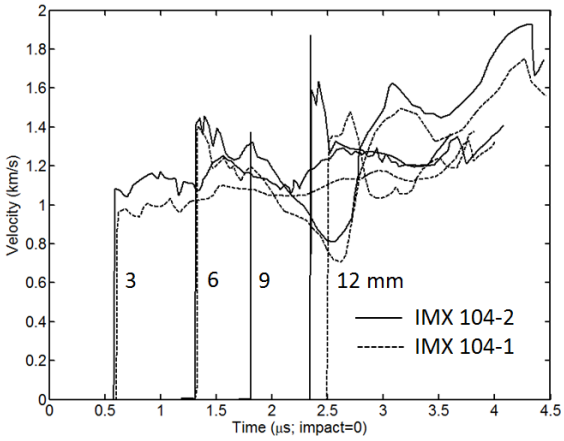

Fig. 6. Waveforms measured by PDV for shots 104-1 and 104-2 (design in Fig. 1).

The final two IMX-104 tests used the improved design shown in Figure 2. Test 104-3 produced the waveforms shown in Fig. 7.

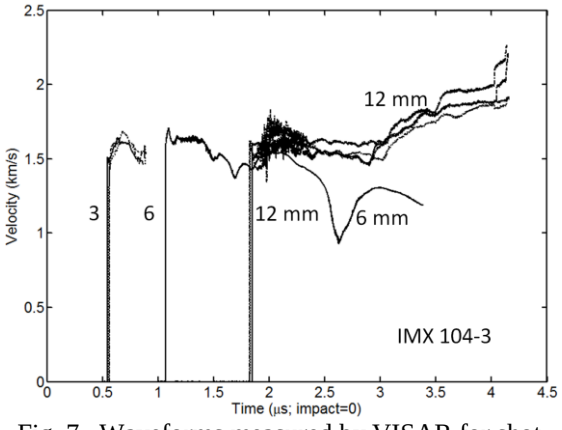

Fig. 7. Waveforms measured by VISAR for shot 104-3 (design in Fig. 2; 14.6 GPa initial loading).

This test used several VISAR probes on different spots for the 3 and 12 mm thick samples, as well as a line-imaging VISAR on the 9 mm sample. Slight variations in the waveforms from one spot to another were observed. For the 3 mm sample (in which the three spots were evenly spaced on a 7.62 mm diameter circle), these are probably related to sample heterogeneities. For the 12 mm sample, the three spots on a 10.16 mm diameter circle appear to show spatial variation in detonation properties. That detonation occurred in this sample is discussed below.

As shown in Fig. 2, 6 small LiF windows were mounted flush with the impact plane and monitored by VISAR to establish the impact timing as a function of position (fit to a functional form $t(x,y) = ax+by+C+Dr^2$). The fit had an RMS value of 1.4 ns, and indicated an unexpectedly large (25 ns ~ 0.045 mm) concave bowing of the impactor. The diagnostics on the earlier tests were not sensitive to this radial dependence.

The line VISAR data showed only the initial arrival on the 9 mm sample; this arrival did not show any spatial variation except a slight tilt consistent with the impact geometry. The surface may have so degraded after impact that the high f-number return optics did not capture the reflected light. This diagnostic was replaced with a single-point VISAR for the remaining shot.

The waveforms for test 104-4 are shown in Fig. 8. Again, some spatial variation is observed for the samples where multiples probes were used (2 each for the 3 and 6 mm samples and 3 for the 12 mm sample). As noted below, there is wavespeed evidence of detonation beginning with the 6 mm thick sample.

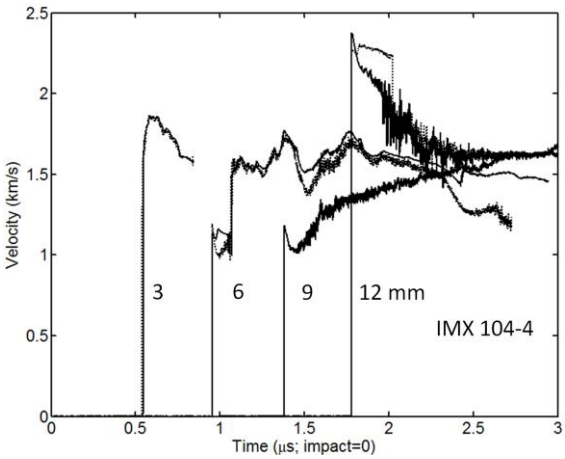

Fig. 8. Waveforms measured by VISAR for shot 104-4 (design in Fig. 2; 15.8 GPa initial loading).

Since the windows have a higher shock impedance than the IMX-101 and IMX-104 samples, the samples were reshocked when the loading wave reflected off of the interface beween the sample and the window. The resulting reshocked states may be calculated from the Hugoniot state, the material velocity of the interface following initial loading, and the known Hugoniots of the window materials. These states are plotted in Fig. 9 and enumerated in Table 4. We are still trying to understand why some of the IMX-104 reshock paths are vertical in this figure.

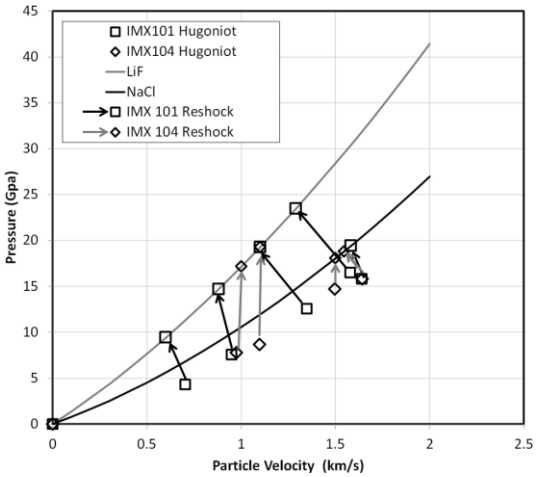

Fig. 9. Reshock paths for all experiments.

Table 4. Reshock values.

Shot	$U_{Plateau}$ km/s	P_{RS} GPa	$U_{P(RS)}$ km/s	ρ_{RS} gm/cc	ε_{RS}
101-1	0.6	9.4	0.8	2.00	0.19
101-2	0.88	14.7	1.06	2.08	0.22
101-3	1.1	19.2	1.62	2.17	0.25
101-4	1.29	23.4	1.99	2.28	0.29
101-5	1.58	19.4	1.58	2.16	0.25
104-1	1.0	17.1	0.95	2.18	0.21
104-2	1.1	19.2	1.07	2.24	0.23
104-3	1.54	18.8	1.45	2.40	0.28
104-4	1.5	18.0	1.79	2.47	0.30

Wavespeeds and Run-to-Detonation

The Hugoniot results above used the wavespeeds from the 3 mm and 6 mm thick samples. It is also interesting to tabulate the wavespeeds observed as the loading wave progresses through different samples. Consider the sketch in Fig. 10. The times-of-arrival of the loading wave at 0, 3, 6, 9 and 12 mm are known for each experiment (with some missing values). It is possible to use the arrival time differences to deduce the wavespeed as the wave travels (e.g.) from 6 to 12 mm.

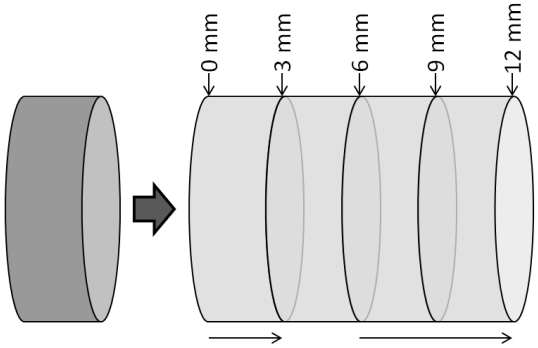

Fig. 10. Schematic of usage of different sample thicknesses to infer wavespeed evolution.

These results are shown in Table 4 below. The wavespeed of detonating IMX-104 is known as ~7.5 km/s., while that for IMX-101 is 6.9 km/s. For the 101, the tabulated wavespeeds indicate velocities lowere than the measured detonation velocity. The waveforms in figures 4 and 5 suggest that detonation may have occurred between 9 and 12 mm for shot 101-4 at 15.8 GPa and between 6 and 9 mm in shot 101-5 at 16.5 GPa. The IMX-104 appears to have detonated at 14 GPa (101-3) at roughly 6 mm run distance and at 15.8 GPa at between 3 and 6 mm run distance. Using the 19-channel interferometer with more finely spaced sample thicknesses is needed to resolve the run-to-detonation distance.

Acknowledgments

Sandia National Laboratories is a multi-program laboratory managed and operated by Sandia Corporation, a wholly owned subsidiary of Lockheed Martin Corporation, for the U.S. Department of Energy's National Nuclear Security Administration under contract DE-AC04-94AL85000. Document # SAND2013-7855.

1. Strand, O.T., et al., *Compact system for high-speed velocimetry using heterodyne techniques.* Review of Scientific Instruments, 2006. **77**(8).
2. Barker, L.M. and R.E. Hollenbach, *Laser interferometer for measuring high velocities of any reflecting surface.* Journal of Applied Physics, 1972. **43**(11): p. 4669.
3. Point of contact is Bruce Marshall, marshabr@ns.doe.gov
4. Lemar, E.R., et al., *Unreacted Hugoniot of Composition B-3 for stresses of 0 - 16 kbar.* Journal of Applied Physics, 1985. **58**(9): p. 3404-3408.
5. Thornhill, T.F., L.C. Chhabildas, and W.D. Reinhart, *Time resolved optical signatures for Hugoniot state measurements in shock compressed Composition-B,* in *Shock Compression of Condensed Matter - 2009, Pts 1 and 2*, M.L. Elert, et al., Editors. 2009, Amer Inst Physics: Melville. p. 404-407.
6. Marsh, S.P., *LASL Shock Hugoniot Data*1980: University of California Press.
7. Stevens, L.L., et al., *The high-pressure phase behavior and compressibility of 2,4,6-trinitrotoluene.* Applied Physics Letters, 2008. **93**(8).

Table 4. Wavespeeds observed for various intervals.

Shot	P_H GPa	Average wavespeeds over intervals noted (km/s)						
		0→12	0→3	3→6	6→9	9→12	0→6	6→12
101-1	4.3	3.78	3.75	3.75	3.93	3.68	3.75	3.80
101-2	7.1	4.77	4.93	4.93	5.36	4.03	4.93	4.61
101-3	12.4	5.63	5.76	5.76	5.65	5.37	5.76	5.51
101-4	15.8	6.11	5.84	5.84	6.26	6.59	5.84	6.42
101-5	16.5	6.35	6.40	6.40	6.59	6.29	6.40	6.43
104-1	7.7	4.68	4.56	4.56	5.14	4.52	4.56	4.72
104-2	8.6	4.94	4.54	4.54	5.88	5.03	4.54	5.42
104-3	14.7	6.49	5.38	6.11	----	----	5.72	7.50
104-4	15.8	6.73	5.55	7.23	6.89	7.65	6.28	7.25